



Journal of Geotechnical and Geoenvironmental Engineering

Technical Papers

- 493 Design Charts for Piles Supporting Embankments on Soft Clay
H. G. Poulos
- 502 Effect of Footing Roughness on Bearing Capacity Factor N_c
Jyant Kumar and K. M. Kouzer
- 512 Numerical Investigation of the Effect of Vertical Load on the Lateral Response of Piles
S. Karthigeyan, V. V. G. S. T. Ramakrishna, and K. Rajagopal
- 522 Case History: Capacity of a Drilled Shaft in the Atlantic Coastal Plain
John F. Pizzi
- 531 Pullout Behavior of Granular Pile-Anchors in Expansive Clay Beds In Situ
A. Srirama Rao, B. R. Phanikumar, R. Dayakar Babu, and K. Suresh
- 539 Simulating Seismic Response of Cantilever Retaining Walls
S. P. G. Madabhushi and X. Zeng
- 550 Hydraulic Conductivity of Geosynthetic Clay Liners Exhumed from Landfill Final Covers
Stephen R. Meer and Craig H. Benson
- 564 Measurement Biases in the Bender Element Test
Y. H. Wang, K. F. Lo, W. M. Yan, and X. B. Dong
- 575 Laboratory Rainfall-Induced Slope Failure with Moisture Content Measurement
Adrin Tohari, Makoto Nishigaki, and Mitsuru Komatsu
- 588 Soil-Water Transfer Mechanism for Solidified Dredged Materials
W. Zhu, C. L. Zhang, and Abraham C. F. Chiu

contents continue on back cover



The Geo-Institute

contents continued from front cover

- 599 Anisotropy-Based Failure Criterion for Interphase Systems
Jianfeng Wang, Joseph E. Dove, and Marte S. Gutierrez

Technical Notes

- 609 Unit Weight Determination of Landfill Waste Using Sonic Drilling Methods
Michael J. Burlingame, Dincer Egin, and William B. Armstrong

Discussions and Closures

- 613 Discussion of "Determination of Atterberg Limits: Uncertainty and Implications" by Alvaro Gutiérrez
Yakov M. Reznik
- 614 Closure by *Alvaro Gutiérrez*
- 614 Discussion of "Suction Stress Characteristics Curve for Unsaturated Soil" by Ning Lu and William J. Likos
T. S. Nagaraj, T. Schanz, and Prasad K. Nagendra

Errata

- 617 Errata for "Threshold Shear Strain for Cyclic Pore-Water Pressure in Cohesive Soils" by Chu-Chung Hsu and Mladen Vucetic
Chu-Chung Hsu and Mladen Vucetic

ASCE
American Society
of Civil Engineers

1801 Alexander Bell Drive
RESTON, VA 20191-4400



1090-0241(200705)133:5;1-A

Board Publications Committee

Andrew W. Herrmann, P.E., F.ASCE, *Chair*
Kenneth L. Carper, M.ASCE
Gregory E. DiLoreto, P.E., L.S., F.ASCE
William M. Hayden Jr., Ph.D., P.E., F.ASCE
Thomas M. Rachford, Ph.D., P.E., F.ASCE
Robert H. Wortman, Ph.D., M.ASCE
Bruce Gossett, Aff.M.ASCE, *ASCE Staff Contact*

Publications

Bruce Gossett, *Managing Director and Publisher*

Journals Department

Johanna M. Reinhart, *Director, Journals*
Jackie Perry, *Managing Editor, Journals*
Holly Koppel, *Discussions and Closures*

Production Department

Charlotte McNaughton, *Director, Production*
Teresa Metcalfe, *Manager, Journals Production*
Gene Sullivan, *Senior Production Editor*
Nancy Green, *Production Editor*
Rajashree Ranganathan, *Production Editor*
Xi Van Fleet, *Manager, Information Services*
Donna Dickert, *Reprints*

Publishing Office

Journals Department
ASCE
1801 Alexander Bell Drive
Reston, VA 20191-4400
Telephone: (703) 295-6290
E-mail: journal-services@asce.org

Journal of Geotechnical and Geoenvironmental Engineering

VOLUME 133 / NUMBER 5

MAY 2007

Technical Papers

- 493 Design Charts for Piles Supporting Embankments on Soft Clay
H. G. Poulos
- 502 Effect of Footing Roughness on Bearing Capacity Factor N_y
Jyant Kumar and K. M. Kouzer
- 512 Numerical Investigation of the Effect of Vertical Load on the Lateral Response of Piles
S. Karthigeyan, V. V. G. S. T. Ramakrishna, and K. Rajagopal
- 522 Case History: Capacity of a Drilled Shaft in the Atlantic Coastal Plain
John F. Pizzi
- 531 Pullout Behavior of Granular Pile-Anchors in Expansive Clay Beds In Situ
A. Srirama Rao, B. R. Phanikumar, R. Dayakar Babu, and K. Suresh
- 539 Simulating Seismic Response of Cantilever Retaining Walls
S. P. G. Madabhushi and X. Zeng
- 550 Hydraulic Conductivity of Geosynthetic Clay Liners Exhumed from Landfill Final Covers
Stephen R. Meer and Craig H. Benson
- 564 Measurement Biases in the Bender Element Test
Y. H. Wang, K. F. Lo, W. M. Yan, and X. B. Dong
- 575 Laboratory Rainfall-Induced Slope Failure with Moisture Content Measurement
Adrin Tohari, Makoto Nishigaki, and Mitsuru Komatsu
- 588 Soil-Water Transfer Mechanism for Solidified Dredged Materials
W. Zhu, C. L. Zhang, and Abraham C. F. Chiu
- 599 Anisotropy-Based Failure Criterion for Interphase Systems
Jianfeng Wang, Joseph E. Dove, and Marte S. Gutierrez

Technical Notes

- 609 Unit Weight Determination of Landfill Waste Using Sonic Drilling Methods
Michael J. Burlingame, Dincer Egin, and William B. Armstrong

Discussions and Closures

- 613 Discussion of "Determination of Atterberg Limits: Uncertainty and Implications" by Alvaro Gutiérrez
Yakov M. Reznik
- 614 Closure by *Alvaro Gutiérrez*

- 614 Discussion of "Suction Stress Characteristics Curve for Unsaturated Soil" by
Ning Lu and William J. Likos
T. S. Nagaraj, T. Schanz, and Prasad K. Nagendra

Errata

- 617 Errata for "Threshold Shear Strain for Cyclic Pore-Water Pressure in
Cohesive Soils" by Chu-Chung Hsu and Mladen Vucetic
Chu-Chung Hsu and Mladen Vucetic

Soil–Water Transfer Mechanism for Solidified Dredged Materials

W. Zhu¹; C. L. Zhang²; and Abraham C. F. Chiu³

Abstract: The paper presents a study of the soil–water transfer mechanism for solidified dredged materials. Soil–water consists of free water, bound water, and hydration water. The resulting hydrates change the soil–water composition in a cement-based solidification process. A soil–water transfer model is postulated to explain the relationship between soil–water composition and cement content. The test results of solidified specimens cured after 7 and 28 days showed that the hydration water increases linearly with the cement content, and the bound water increases nonlinearly with the cement content. There exists a threshold cement content beyond which the free water is eliminated from the solidified specimen. Further, the model is used to predict the mechanical behavior of the solidified dredged materials. Below the threshold cement content, the unconfined compressive strength may be related to the bound water content. Above the threshold cement content, the shear strength may be related to the hydration water content. In addition, brittle stress-strain behavior commences when the incremental increase of bound water content begins decreasing.

DOI: 10.1061/(ASCE)1090-0241(2007)133:5(588)

CE Database subject headings: Dredging; Cement; Solidification; Pore water; Compressive strength.

Introduction

Dredging is necessary to keep harbors and waterways navigable, to prevent rivers from flooding, and to restore the ecosystem of degenerative water bodies (Winkels and Stein 1997; Forstner and Calmano 1998). Existing disposal techniques for dredged material (DM) have concentrated on ocean and land disposal. In recent years over 100×10^6 m³ of DM were disposed annually into the ocean in China (Zhang et al. 2004). However, the presence of contaminants has generated concern about ocean disposal as such operations may pose a potential threat to water quality and aquatic life. Moreover, increasing pressure from urbanization leads to a rapid reduction of available on-land disposal sites. Thus, utilization of DM for beneficial uses such as fill is being considered to reduce the need for new disposal areas.

In general, DM are very soft soils which have very low shear strengths ($c_u < 50$ kPa) and natural water contents higher than their liquid limits. Cement-based solidification is one of the technologies used to convert the semi-solid materials into monolithic solids. Cement is used as a binding agent and mixed with the DM to produce a mechanically stable soil matrix. The general objec-

tives of solidification are to increase the strength and stiffness, reduce free liquids, and immobilize possible contaminants (Mitchell 1981; Meegoda et al. 2000).

The mechanical properties of the solidified (or cement) soft soil have been extensively studied in the past (Connor 1990; Nagaraj et al. 1996; Tatsuoka et al. 1997; Tremblay et al. 2001; Dermatas et al. 2003a,b; Lee et al. 2005; Horpibulsuk et al. 2005). Many studies have focused on the influence of cement content or water–cement ratio on the strength and stiffness of the solidified soil (Lee et al. 2005; Horpibulsuk et al. 2005); few focus on the mechanism of solidification. Microstructural studies of solidified soils reveal that their behavior is governed primarily by the hydrates (Locat et al. 1996; Rao and Rajasekaran 1996; Dermatas et al. 2003a,b; Chew et al. 2004). Hydrates are the reaction products between cement, clay minerals in the soil, and water. In general, the microstructure of the hydrates can be qualitatively investigated and identified by methods such as scanning electron microscopy and X-ray diffractometry (XRD). However, it is difficult to identify the hydrates by performing the XRD analysis because the soil minerals normally dominate the diffraction patterns and the characteristic Bragg angles of the hydrates are concentrated around the low angle regime (Taylor 1997; Dermatas et al. 2003a). In addition, the existing qualitative XRD analyses only yield information on the crystalline phases present in the material. The possibility of significant amorphous content in the solidified soil cannot be ruled out. This material may have a profound effect on the physical properties of the solidified soil. Thus, there is a need for a simple and practical method which can reflect the contribution of the hydrates in the solidified soil matrix.

The solidification of the cement treated DM involves the following: (1) the hydration of the cement; (2) the pozzolanic reactions of the clay minerals in the DM; and (3) the interaction between the resulting hydrates and soil particles (Connor 1990; Taylor 1997). Table 1 shows the major chemical reactions involved in the solidification process. The principal reaction is the hydration of the cement. The major hydrates formed are calcium silicate hydrate (CSH), calcium aluminate hydrate (CAH), and

¹Professor, State Key Laboratory of Hydrology, Water Resources and Hydraulic Engineering, Hohai Univ., Nanjing 210098, China. E-mail: weizhu@jlonline.com

²Postgraduate Student, College of Environmental Science and Engineering, Hohai Univ., Nanjing 210098, China. E-mail: zhangchunlei@mail.edu.cn

³Associate Professor, Geotechnical Research Institute, Hohai Univ., Nanjing 210098, China. E-mail: acfchiu@yahoo.com.cn

Note. Discussion open until October 1, 2007. Separate discussions must be submitted for individual papers. To extend the closing date by one month, a written request must be filed with the ASCE Managing Editor. The manuscript for this paper was submitted for review and possible publication on August 25, 2005; approved on November 14, 2006. This paper is part of the *Journal of Geotechnical and Geoenvironmental Engineering*, Vol. 133, No. 5, May 1, 2007. ©ASCE, ISSN 1090-0241/2007/5-588–598/\$25.00.

Table 1. Chemical Reactions during Solidification

Reactions	Chemical formulas
Hydration reactions of portland cement (Lea 1970)	$2(3\text{CaO}\cdot\text{SiO}_2)+5.5\text{H}_2\text{O}\rightarrow 3\text{CaO}\cdot 2\text{SiO}_2\cdot 2.5\text{H}_2\text{O}+3\text{Ca}(\text{OH})_2$ tricalcium silicate CSH
	$2(2\text{CaO}\cdot\text{SiO}_2)+3.5\text{H}_2\text{O}\rightarrow 3\text{CaO}\cdot 2\text{SiO}_2\cdot 2.5\text{H}_2\text{O}+\text{Ca}(\text{OH})_2$ bicalcium silicate CSH
	$3\text{CaO}\cdot\text{Al}_2\text{O}_3+12\text{H}_2\text{O}+\text{Ca}(\text{OH})_2\rightarrow 4\text{CaO}\cdot\text{Al}_2\text{O}_3\cdot 13\text{H}_2\text{O}$ tricalcium aluminate CAH
	$3\text{Ca}(\text{OH})_2\rightarrow \text{Ca}^{2+}+2\text{OH}^-$ $\text{Ca}^{2+}+2\text{OH}^-+\text{SiO}_2$ (clay silica) \rightarrow CSH $\text{Ca}^{2+}+2\text{OH}^-+\text{Al}_2\text{O}_3$ (clay alumina) \rightarrow CAH
Pozzolanic reactions	

hydrated lime (calcium hydroxide). Secondary pozzolanic reactions also take place between the hydrated lime and the leachable silica and alumina from the clay minerals in the DM to form additional CSH and CAH. The extent of the pozzolanic reactions depends on the activity of the clay minerals (e.g., kaolinite is more inert than montmorillonite). It is shown in Table 1 that the water consumption is proportional to the resultant hydrates in the hydration reactions. In addition, CSH and CAH have very high specific surface areas with irregular hydrogen bonding which can attract water molecules around its vicinity. Hence, the development of the hydrates within the soil matrix may alter its soil-water composition.

Based on the binding forces acting on the water molecules in the soil matrix, soil-water can be classified into: (1) hydration water; (2) bound water; and (3) free water (Mitchell and Soga 2005). Hydration water (HW) is chemically bound water which is an integral part of soil minerals. Bound water (BW) refers to those water molecules physically bound in the vicinity of soil particles (double layer) by adhesive forces. Free water (FW) is the loosely held water which is controlled by surface tensional forces and gravity. In conventional soil mechanics, pore water (PW) in the soil matrix is comprised of BW and FW.

Fig. 1 shows the schematic diagram for the soil-water transfer mechanism during solidification. The initial masses of FW, BW, HW, and PW per unit volume of the pretreated soil are represented by m_{fw0} , m_{bw0} , m_{hw0} , and m_{pw0} , respectively, where m_{pw0} =sum of m_{fw0} and m_{bw0} . After adding the cement, the masses of FW, BW, and PW per unit volume of the solidified soil are represented by m_{fw} , m_{bw} , and m_{pw} , respectively, where m_{bw} =sum of m_{bw0} and Δm_{bw} ; and m_{pw} =sum of m_{fw} and m_{bw} .

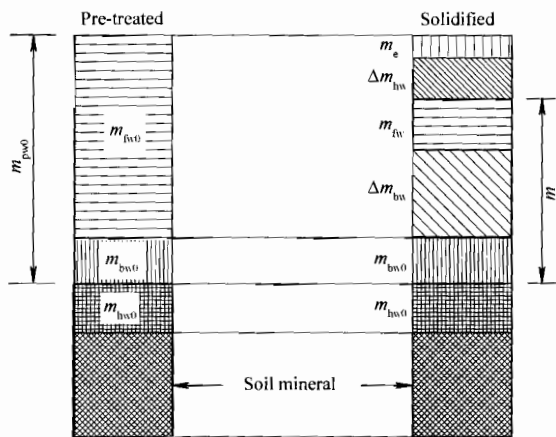


Fig. 1. Schematic diagram for soil-water transfer mechanism during solidification

During cement hydration, there is a loss of PW. The hydration reactions consume part of the PW which becomes the HW bounded into the newly formed hydrates. In addition, some water evaporates by the heat of hydration during the cement reactions. Thus, the loss of PW ($m_{pw0}-m_{pw}$) during solidification is balanced by the following equation:

$$\Delta m_{hw} + m_e = m_{pw0} - m_{pw} \quad (1)$$

where Δm_{hw} and m_e =change in the mass of HW and the mass of water loss in evaporation per unit volume of the solidified soil, respectively; and Δm_{hw} =amount of HW bounded in the hydrates during the cement hydration which may reflect the amount of the products from hydration found in the solidified soil. In addition, part of the PW is transferred to BW because the formation of CSH and CAH which can attract more water around their surface. Thus, the change in BW content (Δm_{bw}) may reflect the extent of the hydrates (products from hydration and pozzolanic reactions) developed in the solidified soil. Thus, knowledge of Δm_{hw} and Δm_{bw} can be used to evaluate the amount and extent of the hydrates developed in the solidified DM.

The composition of FW, BW, and HW in the solidified soil depends on the cement content (a_c). A soil-water transfer model is proposed and shown in Fig. 2. In this model, Δm_{hw} and Δm_{bw} are functions of a_c . It is further assumed that there is a threshold cement content (a_{c0}) beyond which the FW is eliminated. The model assumes that Δm_{hw} increases with a_c and Δm_{bw} increases with a_c for $a_c \leq a_{c0}$. The objectives of this study were to (1) investigate the solidification process of the DM based on the proposed soil-water transfer model and (2) correlate the strength and stress-strain behavior of the solidified DM with the proposed model. In this study, three different DM were treated by cement. After curing the specimens for 7 and 28 days, the soil-water

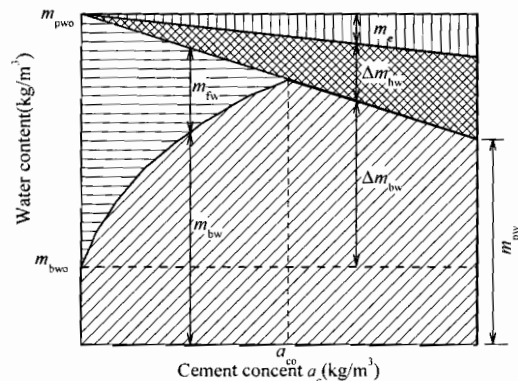


Fig. 2. Soil-water transfer model for solidified soil

Table 2. Basic Physical Properties of DM

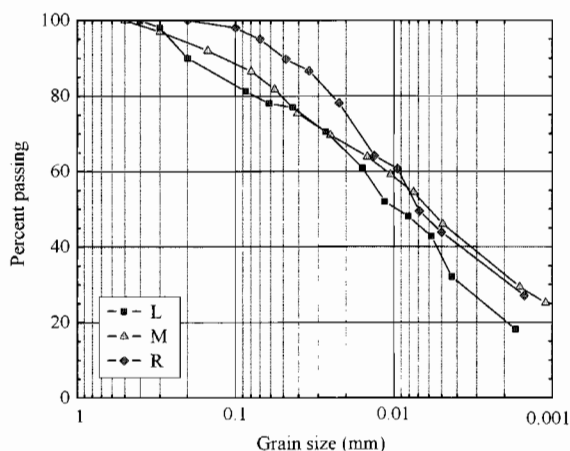
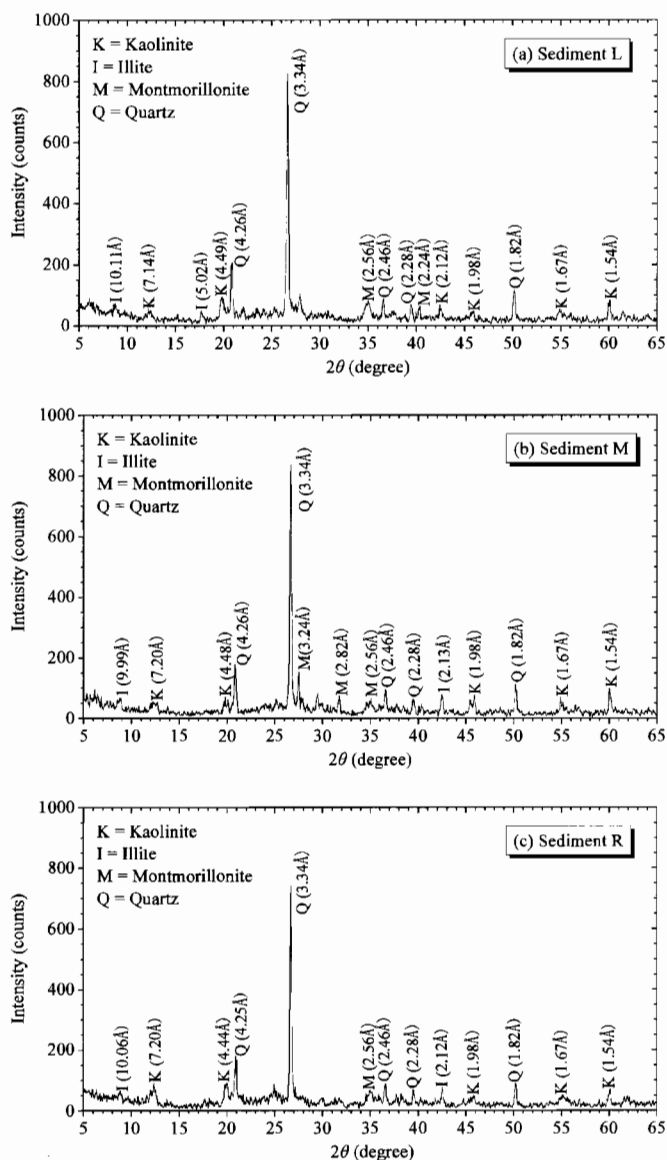
Physical index	L	M	R
Gravimetric water content (%)	108	93	95
Volumetric water content (%)	74.1	71.8	71.7
Liquid limit (%)	75	73	62
Plastic limit (%)	29	32	35
Plastic index	47	41	27
Specific gravity	2.65	2.74	2.67
Bulk unit weight (kN/m ³)	14.0	14.6	14.4
Organic content (%)	0.45	0.31	0.32
Clay content (<2 μm) (%)	20	32	30

composition, unconfined compressive strength, and stress-strain curves were determined. The effects of cement content on soil-water composition, i.e., the water content parameters Δm_{hw} and Δm_{bw} were investigated. Further, correlations between the aforementioned water content parameters and engineering behavior, such as unconfined compressive strength and stress-strain behavior were suggested.

Experimental Studies

Materials

In this study the DM were taken from three different locations in China: (1) a lake sediment (L) from Wuxi; (2) a marine sediment (M) from Shenzheng; and (3) a river sediment (R) from Guangzhou. The basic physical index tests were conducted in accordance with the procedures given in GB/T 50123-1999 (Ministry of Construction P. R. China 1999). The grain size distribution curves were obtained from wet sieving and hydrometer methods. The basic physical properties and the grain size distribution curves of the DM are summarized in Table 2 and Fig. 3, respectively. According to the Unified Soil Classification System, L and M are classified as clay of high plasticity and R is classified as silt of high plasticity. XRD analysis of the untreated DM was carried out by a Rigaku D/max-rC rotating anode X-ray powder diffractometer. Air-dried powdered samples (particle size less than 75 μm) of the untreated DM were used. The X-ray source was a Cu anode operating at 40 kV and 100 mA using Cu K α radiation ($\lambda=1.5406 \text{ \AA}$). The run speed was 3°/min. Data were collected

**Fig. 3.** Grain size distribution curves for untreated DM**Fig. 4.** XRD patterns for untreated DM

between 5 and 65° in 2θ increments (Mitchell and Soga 2005). Mineralogical analysis of X-ray diffraction pattern of the untreated DM was carried out by comparing with the X-ray powder diffraction standard files (Joint Committee for Powder Diffraction Standards 1995). The XRD patterns are shown in Fig. 4, which reveal that kaolinite, illite, and montmorillonite are the predominant clay minerals in the DM. Type I Ordinary Portland cement (OPC) was used as the cementing agent. The chemical composition of the OPC was determined by the ARL-9800 x-ray fluorescence spectrometer and is shown in Table 3.

Specimen Preparation

Water was initially added to the slurries of the three DM in order to achieve similar initial volumetric water contents. The specimens were prepared from mixing the slurries of the DM with dry cement powder. For a unit volume of slurry, seven different cement contents, a_c (50, 100, 200, 300, 400, 500, and 700 kg/m³), were used but the volumetric water content was maintained around 72–74%. Previous studies (Tang et al. 2001) showed that the unconfined compressive strength (q_u) of the solidified DM can

Table 3. Chemical Composition of Type I Ordinary Portland Cement

Chemical property	Percentage
Calcium oxide (CaO)	52.77
Silicon dioxide (SiO ₂)	22.04
Aluminum oxide (Al ₂ O ₃)	13.56
Sulphur trioxide (SO ₃)	4.00
Magnesium oxide (MgO)	3.22
Ferric oxide (Fe ₂ O ₃)	2.34
Potassium oxide (K ₂ O)	0.94
Titanium dioxide (TiO ₂)	0.55
Loss on ignition	0.55

reach up to 1 MPa for a_c of 150 kg/m³ which meets the strength requirement for typical fill materials. Cement contents greater than 150 kg/m³ were also studied in order to find out the threshold cement content (a_{c0}) beyond which FW vanishes. The slurry and cement were mixed thoroughly inside a domestic mixing machine to achieve uniform mixing. The mixing was done as fast as possible to avoid hardening of the cement-soil mixture. Six specimens were prepared for each mix. The mixture was placed into stainless steel molds 39 mm in diameter and 80 mm in height. The mixing and placing was completed at room temperature and took approximately 20 min. The specimens were wrapped by plastic sheet and put inside an environmental chamber for curing where the ambient temperature and relative humidity were maintained at 20±2°C and higher than 90%, respectively. After curing the specimens for 7 and 28 days, unconfined compressive strengths, PW and BW contents of the specimens were determined.

As the cement reactions are exothermic, a control experiment was conducted by monitoring the loss of water due to evaporation during mixing at room temperature and curing inside the environmental chamber. It was found that most of the evaporated water was driven off during the mixing at room temperature and the average value was 12 kg/m³ for a_c ranging from 50 to 700 kg/m³. Then the water which evaporated inside the environmental chamber reached a steady value after curing the specimens for about 7 days and the average value was 1 kg/m³. Thus m_c was estimated as 13 kg/m³ for all specimens in this study.

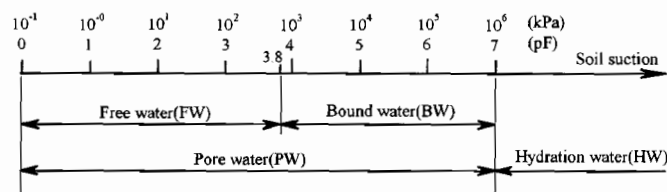
Unconfined Compression Tests

After the designated curing time (7 or 28 days) had elapsed, the specimens were tested for unconfined compressive strength (q_u) at a deformation rate 1.15 mm/min. During each compression test, the specimen was covered by a rubber membrane to minimize water loss due to evaporation. The tests were terminated when the peak strength was attained or 5% axial strain was reached for specimens exhibiting contractive behavior.

Water Contents Determination

Oven Drying Method

After finishing the unconfined compression tests, a minimum of 30 g of soil was taken from each specimen to determine the PW contents (m_{pw} and m_{pw0}). The soil was oven dried to 105°C until reaching a steady mass. The drying process normally lasted for 24 h. m_{pw} was determined from the measurement of the untreated specimen.

**Fig. 5.** Classification of soil-water based on soil suction

Centrifuge Method

The distinction between BW and FW is not well defined. Fig. 5 shows the classification of soil-water according to the soil suction. pF is defined as $-\log(h)$, where h = water head (cm). In soil science, Lebedev (1936) suggested to use a pF of 3.8 to distinguish between BW and FW. The centrifuge method (Gardner 1937) was used to determine the BW contents (m_{bw} and m_{bw0}).

A commercially available Hitachi CR21 small-scale centrifuge with an operable radius of 98 mm was used in the study. The diameter and height of the specimen holder is 50 and 51 mm, respectively. Fig. 6 demonstrates the principles used in the centrifuge method for applying soil suction on a soil specimen. A high gravity field is applied to a soil specimen in the centrifuge. The base of the specimen is treated as the reference free water surface. Gardner (1937) proposed the following equation to calculate the suction in the soil specimen in a centrifuge:

$$\psi = \frac{\rho\omega^2}{2}(r_1^2 - r_2^2) \quad (2)$$

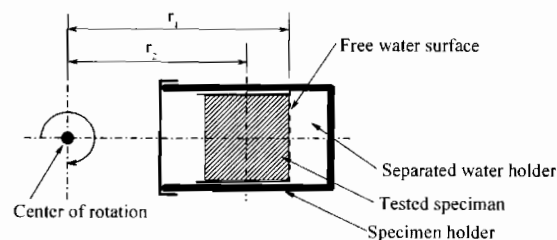
where ψ = suction in the soil specimen (N/m²); r_1 = radial distance to the midpoint of the soil specimen (m); r_2 = radial distance to the free water surface (m); ω = angular velocity (s⁻¹); and ρ = density of the pore fluid (kg/m³). Eq. (2) shows that the applied soil suction is a function of the angular velocity.

In the trial run, a test duration of 180 min is sufficient for the specimen to attain equilibrium condition. All tests were conducted at a controlled temperature of 20°C. After finishing the unconfined compression tests, four specimens for each mix were used for the centrifuge tests. The specimens in the centrifuge were subjected to angular velocities of 6,000–9,000 rpm, which correspond to pFs in the order of 3.5–4, respectively. The BW content at a pF of 3.8 was determined by linear interpolation.

Results and Discussion

Transfer of HW during Solidification

Fig. 7 shows the variation of PW content (m_{pw}) with cement content (a_c) in the solidified DM after 7 and 28 days of curing. The cement and water contents are expressed in mass per unit

**Fig. 6.** Basic principles for centrifuge test

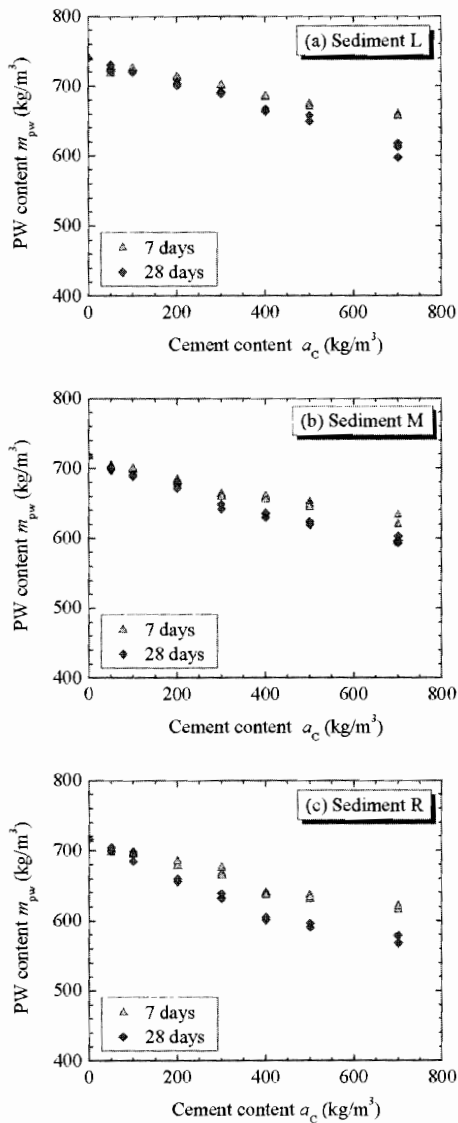


Fig. 7. Effect of cement content on PW content in solidified DM

volume (kg/m^3) because the treatment of DM is based on the volumetric calculation. Fig. 7 shows that m_{pw} decreases linearly with a_c for all three DM. In addition, m_{pw} decreases with increasing curing time. From Eq. (1), there are two probable contributions to the reduction of the PW: (1) The water consumption in hydration reactions (Δm_{hw}) and (2) the loss of water due to evaporation (m_e). As discussed in the previous section, the average value of m_e was estimated as $13 \text{ kg}/\text{m}^3$ for a_c ranging from 50 to $700 \text{ kg}/\text{m}^3$. m_{pw0} is related to the initial volumetric water content of the untreated DM (see Tables 2 and 4). Thus Δm_{hw} is determined from Eq. (1) by subtracting m_{pw0} with m_{pw} and m_e . The variation of the change in HW content (Δm_{hw}) with a_c are shown in Fig. 8. A linear relationship emerged between Δm_{hw} and a_c

$$\Delta m_{hw} = k_1 \times a_c \quad (3)$$

where k_1 =gradient of the linear relationship shown in Fig. 8, which reflect the extent of hydration reactions in the solidified DM. The values of k_1 are summarized in Table 4. It is evident that k_1 increases with the curing time. After 28 days of curing, the values of k_1 are 0.16, 0.16, and 0.21 for L, M, and R, respectively. Hence, the rate of hydration in R is faster than that in L and M.

Table 4. Parameters for the Soil-Water Transfer Model; Days of Curing=7 and 28

Parameter	L		M		R	
	7	28	7	28	7	28
m_{pw0} (kg/m^3)	741	741	718	718	717	717
m_{bw0} (kg/m^3)	262	262	212	212	245	245
k_1 (—)	0.10	0.16	0.12	0.16	0.13	0.21
k_2 (m^3/kg)	0.004	0.006	0.006	0.009	0.006	0.008
k_3 (kg/m^3)	500	500	500	500	500	500

Based on the chemical analysis of cement hydration, the water consumption is approximately 0.2–0.25 of a_c (Lea 1970). Thus it is postulated that the hydration reactions may be far from completed after 28 days of curing in the specimens of L and M. Further study is required to understand how the mineral composition may affect the rate of hydration in the DM.

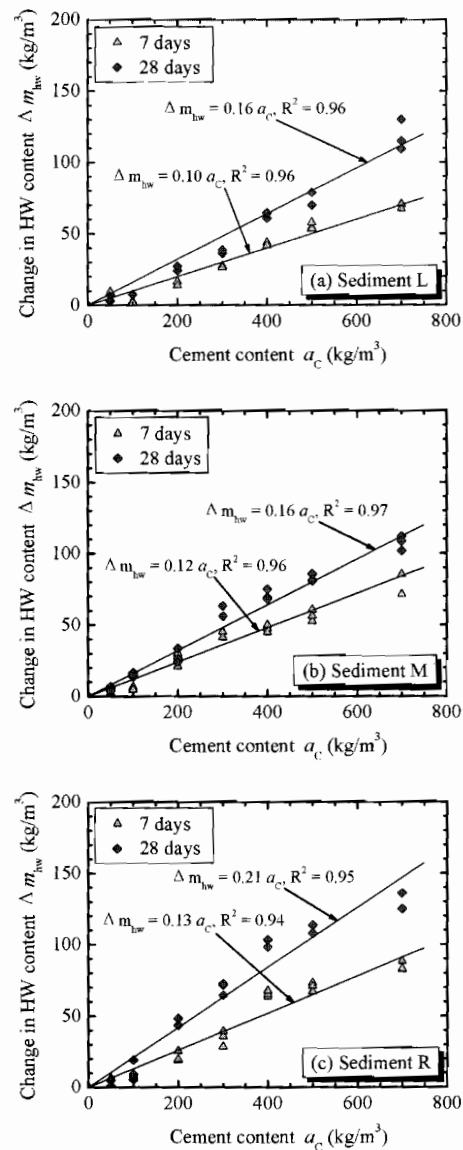


Fig. 8. Effect of cement content on change in HW content in solidified DM

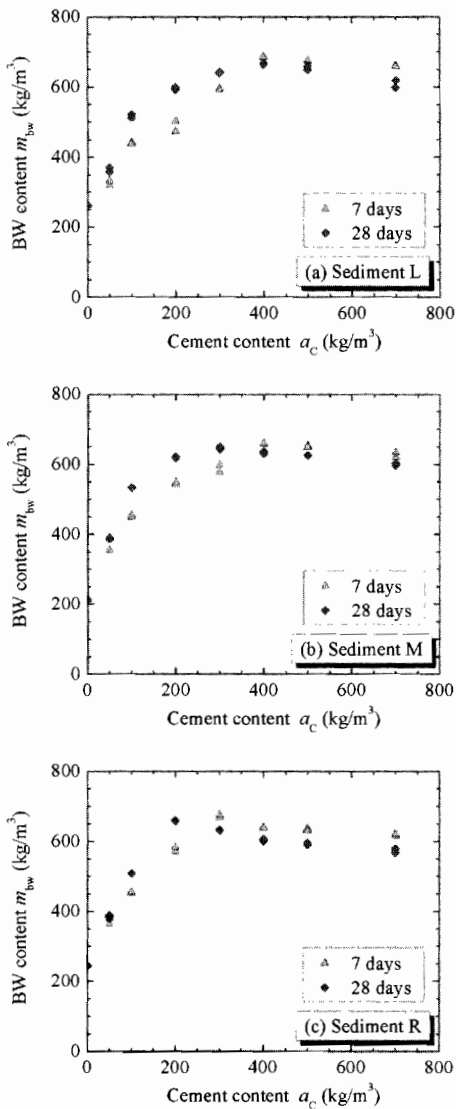


Fig. 9. Effect of cement content on BW content in solidified DM

Transfer of BW during Solidification

Fig. 9 gives the relationship between BW content (m_{bw}) and a_c in the solidified DM after 7 and 28 days of curing. All three DM have different initial BW contents (m_{bw0}), which may reflect the different mineral compositions of the three untreated DM. The values of m_{bw0} are 262, 212, and 245 kg/m^3 , for L, M, and R, respectively. The change in BW content (Δm_{bw}) is obtained by subtracting m_{bw} with m_{bw0} . Fig. 10 shows the variation of Δm_{bw} with a_c . It is found that for $a_c \leq 100 \text{ kg/m}^3$, Δm_{bw} increases linearly with a_c for all three DM. The incremental increase of Δm_{bw} begins decreasing as a_c increases beyond 100 kg/m^3 . It is evident that Δm_{bw} approaches a peak value at a threshold cement content (a_{c0}). Beyond a_{c0} no FW is available as discussed later. In general a_{c0} reduces with increasing curing time. On the other hand, Δm_{bw} increases with the curing time for $a_c < a_{c0}$. The relationship between Δm_{bw} and a_c for $a_c = a_{c0}$ can be expressed by the following expression:

$$\Delta m_{bw} = k_2 (1 - e^{-k_2 a_c}) \quad (4)$$

where k_2 = parameter which controls the rate of increase in Δm_{bw} , i.e., the development of the hydrates within the soil matrix; and k_3 = fictional value of Δm_{bw} at $a_c > a_{c0}$. As the maximum values of

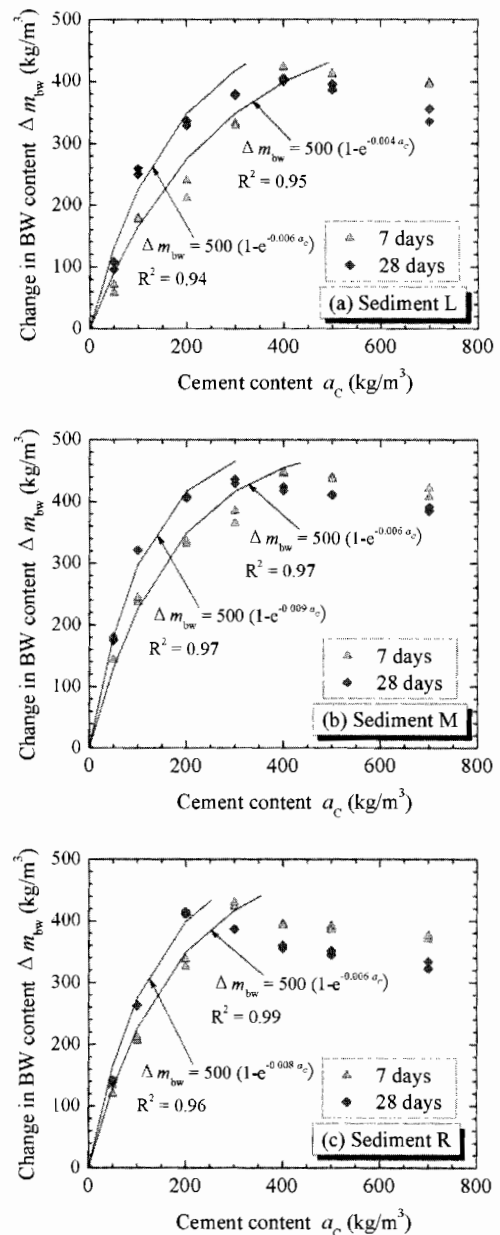


Fig. 10. Effect of cement content on change in BW content in solidified DM

Δm_{bw} are between 390 and 450 kg/m^3 , a reasonable estimation of k_3 is 500 kg/m^3 . The values of k_2 for the three DM are summarized in Table 4. It is evident that k_2 increases with the curing time. Among the three DM, L has the smallest k_2 and M and R have similar values of k_2 . It will be shown in the coming section that m_{bw} equals to m_{pw} for $a_c > a_{c0}$.

Soil-Water Composition in Solidified DM

Fig. 11 shows the variation of soil-water composition with a_c in the solidified DM after 7 and 28 days of curing. All three DM exhibit similar pattern for the soil-water composition which is in good agreement with the proposed soil-water transfer model shown in Fig. 2. The PW content (m_{pw}) decreases linearly with a_c . The reduction of m_{pw} is assumed to transfer partly into HW during cement hydration (Δm_{hw}) and partly loss in evaporation (m_e). m_{pw} is determined by substituting Eq. (3) into Eq. (1)

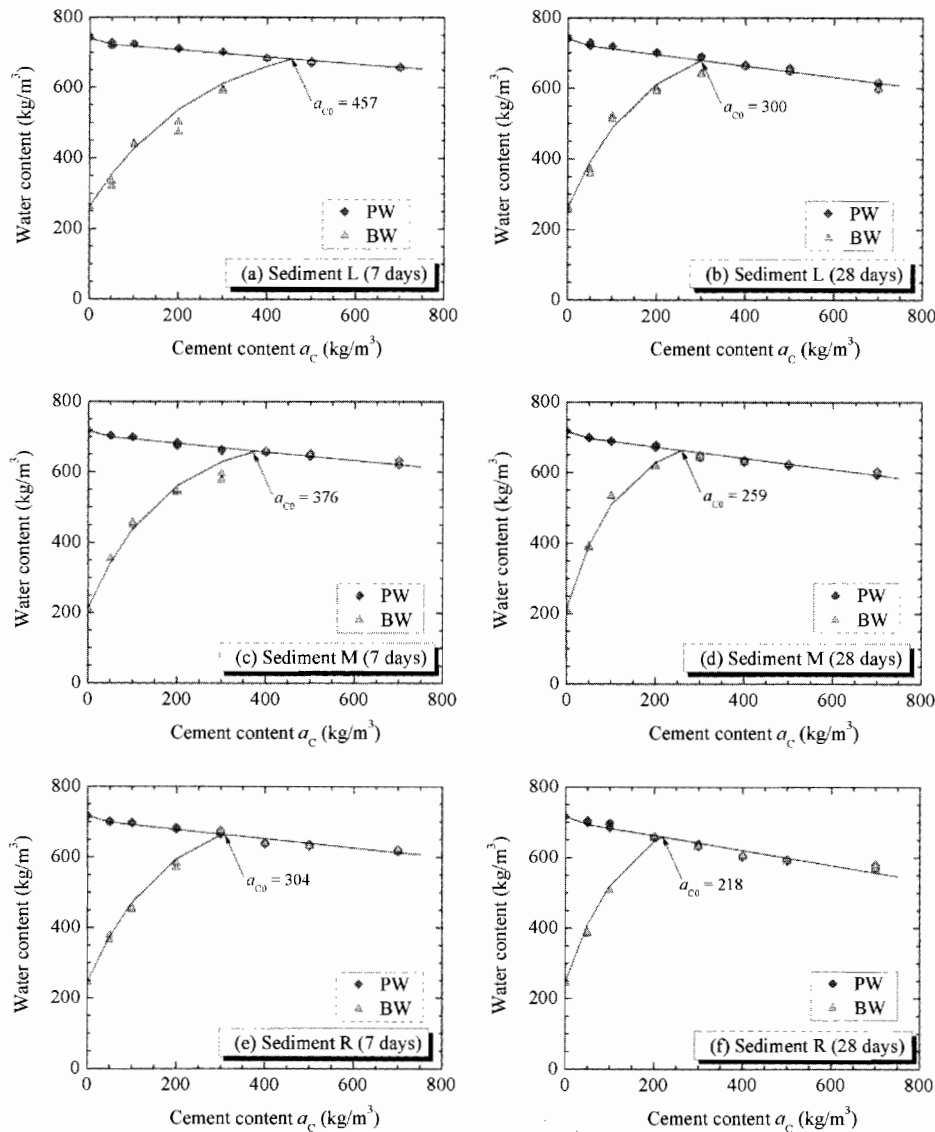


Fig. 11. Effect of cement content on soil–water composition in solidified DM

$$m_{pw} = m_{pw0} - k_1 a_c - m_e \quad (5)$$

The BW content (m_{bw}) increases nonlinearly with a_c , which indicates the increasing extent of the gel form CSH and CAH hydrates developed within the solidified soil matrix. m_{bw} is evaluated by the following equations:

$$m_{bw} = \begin{cases} m_{bw0} + k_3(1 - e^{-k_2 a_c}) & \text{for } a_c \leq a_{c0} \\ m_{pw} & \text{for } a_c > a_{c0} \end{cases} \quad (6a)$$

$$m_{bw} = m_{pw} \quad \text{for } a_c > a_{c0} \quad (6b)$$

a_{c0} = threshold cement content beyond which the FW is eliminated and it is the intersection point of Eqs. (5) and (6a). The FW content (m_{fw}) is calculated by subtracting Eq. (6a) or (6b) from Eq. (5). In this model the soil–water composition is controlled by five parameters: m_{pw0} , m_{bw0} , k_1 , k_2 , and k_3 , where m_{pw0} and m_{bw0} = initial PW and BW content, respectively; k_1 and k_2 govern the rate of increment in HW and BW, respectively. k_3 = fictional value of Δm_{bw} at $a_c > a_{c0}$ which is taken as 500 kg/m^3 in this study. Table 4 summarizes the values of parameters for the three DM used in this study. It is evident that parameters k_1 and k_2 increase with the curing time.

Implications to Mechanical Behavior of Solidified Sediments

Stress–Strain Relationship

Fig. 12 shows the stress–strain curves obtained from unconfined compression tests for a_c of 50, 100, and 200 kg/m^3 . It is evident that ductile behavior is observed for a_c of 50 kg/m^3 . As a_c increases beyond 100 kg/m^3 , the solidified specimens become more brittle with a defined peak strength. Chew et al. (2004) suggested that the increase in the brittleness of the solidified DM is caused by the formation of structure within the solidified soil matrix. When the CSH and CAH gels are formed around the soil particles, more FW are drawn towards the resultant hydrates. As a result the potential of the PW is altered, some portions of FW become BW, and Δm_{bw} commences to increase. Hence, Δm_{bw} may be an appropriate indicator which reflects the structure formed by the interaction of the hydrates and soil particles in the solidified soil. Fig. 10 shows that the increase in Δm_{bw} becomes nonlinear at cement contents of approximately 100 kg/m^3 . Based on the limited experimental data, it seems that the brittle behavior

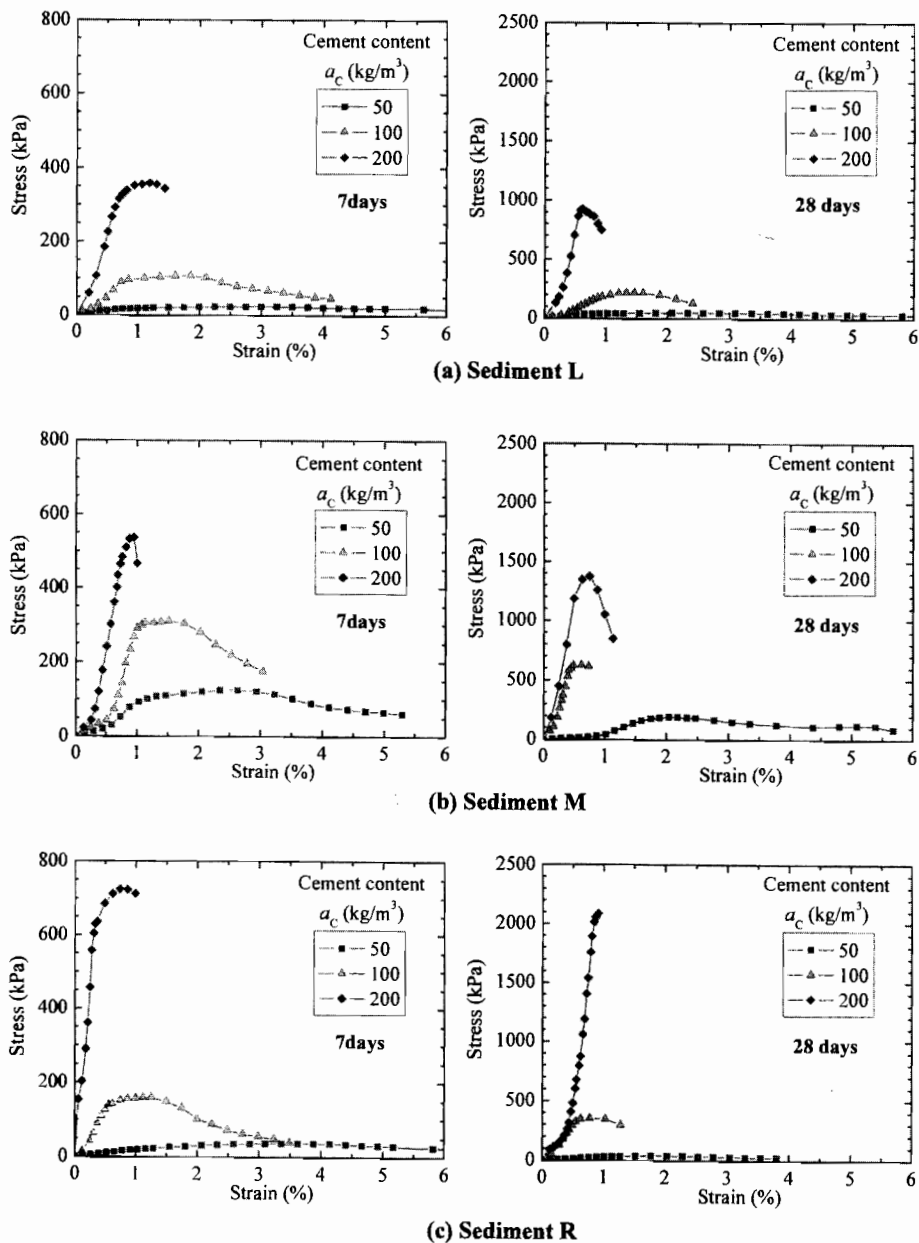


Fig. 12. Stress-strain relationships of solidified DM

commences when the incremental increase of Δm_{bw} begins decreasing, i.e., the derivative of Δm_{bw} with respect to a_c becomes negative. As the extent of the structures continues to develop by adding more cement, it is getting more difficult to draw additional FW toward the hydrates. Hence a reduction in the incremental increase of Δm_{bw} may signify a certain extent of structures developed in the soil matrix.

Unconfined Compressive Strength

Fig. 13 shows the relationships between unconfined compressive strength (q_u) and a_c for the solidified DM after 7 and 28 days of curing. A minimum cement content (a_{cm}) is required before the strength improvement becomes apparent. The values of a_{cm} range from 30 to 70 kg/m^3 for the three DM used in the study. Beyond

a_{cm} , q_u increases nonlinearly with a_c . In addition, q_u increases with the curing time for a given a_c .

As discussed in the previous sections, Δm_{hw} increases with a_c (see Fig. 8) and Δm_{bw} increases with a_c for $a_c = a_{c0}$ (see Fig. 10). In addition, both parameters increase with the curing time for a given a_c . It seems that Δm_{hw} and Δm_{bw} may correlate to q_u . Figs. 14 and 15 show the relationships of Δm_{hw} and q_u , and Δm_{bw} and q_u , for $a_c < a_{c0}$, respectively. The following empirical expressions can be obtained:

$$q_u = \begin{cases} 39.5(\Delta m_{hw} - 0.76) & (7) \\ 9.5(e^{0.013\Delta m_{bw}} - 1) & (8) \end{cases}$$

Δm_{hw} increases linearly with q_u , in other words, q_u is proportional to the amount of hydrates formed from the hydration reactions. In addition, Δm_{bw} increases nonlinearly with q_u and the gradient of

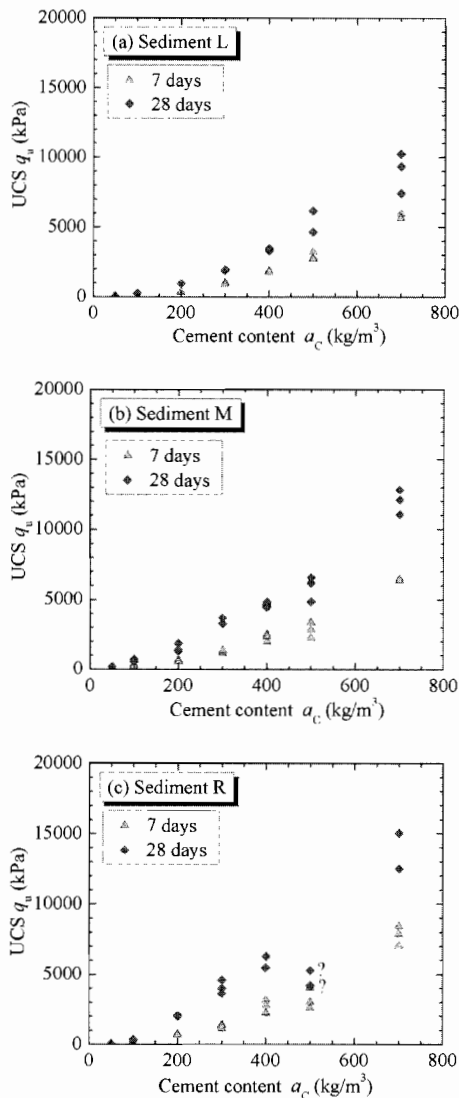


Fig. 13. Effect of cement content on UCS of solidified DM

the curve increases substantially around Δm_{bw} of 200 kg/m^3 , which corresponds to the linear limit of the relationship between Δm_{bw} and a_c (see Fig. 10). As discussed previously this linear limit may be used to indicate the onset of brittle behavior of the solidified DM which is consistent with a significant increase in the corresponding q_u . The coefficients of correlation (R^2) for Eqs. (7) and (8) are 0.84 and 0.93, respectively. It seems that reasonable correlations can be obtained between q_u and the water content parameters Δm_{hw} and Δm_{bw} for $a_c < a_{c0}$. Fig. 16 shows the relationship of Δm_{hw} and q_u for a_c ranging from 50 to 700 kg/m^3 . It should be noted that the measurements at a_c of 500 kg/m^3 for the specimens of R were not used in the data analysis because of unexpected low values of q_u [see the question marks in Figs. 13(c) and 16]. The following empirical expression can be obtained:

$$q_u = 0.14 \Delta m_{hw}^{2.39} \quad (9)$$

R^2 for Eq. (9) is 0.82 which is similar to those of Eqs. (7) and (8). It is proposed that q_u may be correlated to either Δm_{bw} or Δm_{hw} for $a_c < a_{c0}$ and to Δm_{hw} for $a_c > a_{c0}$.

Conclusions

A study of the soil-water transfer mechanism for the solidified DM is presented. Soil-water consists of pore water (free water and bound water) and hydration water. In a cement-based solidification process, the formation of hydrates converts part of the free water to the hydration water which is chemically bound within the structure of the hydrates. In addition part of the free water is transferred to the bound water which is physically bound to gel-form hydrates.

Type 1 Ordinary Portland cement was used to solidify three different DM, from which the effects of cement content (a_c) on

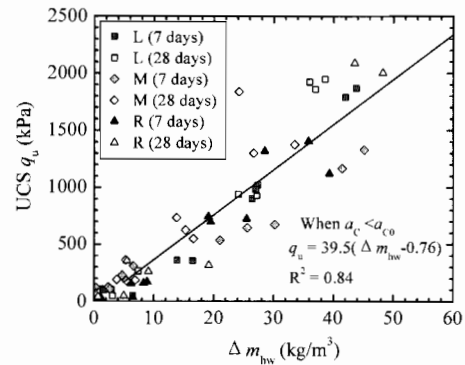


Fig. 14. Effect of change in HW content on UCS of solidified DM for $a_c < a_{c0}$

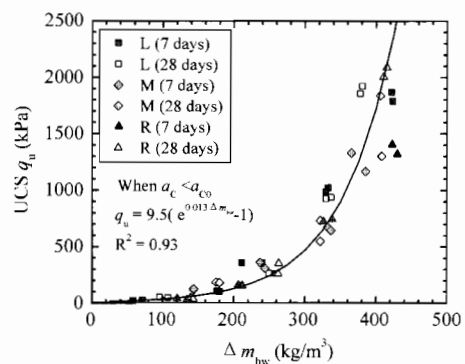


Fig. 15. Effect of change in BW content on UCS of solidified DM for $a_c < a_{c0}$

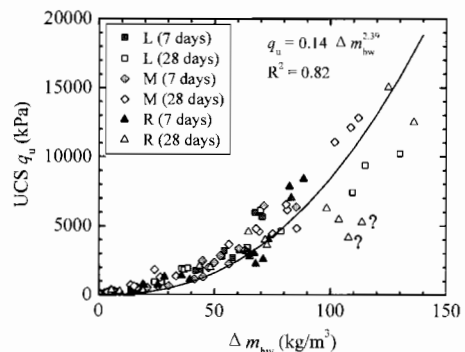


Fig. 16. Effect of change in HW content on UCS of solidified DM for a_c ranging from 50 to 700 kg/m^3

the soil–water composition were studied. The test results of specimens cured after 7 and 28 days showed that: (1) the change in hydration water content (Δm_{hw}) increases linearly with a_c and the ratio of Δm_{hw} to a_c indicates that complete hydration does not take place and (2) the change in bound water content (Δm_{bw}) increases nonlinearly with a_c and its maximum value occurs at a threshold cement content (a_{c0}) beyond which all free water is eliminated.

A soil–water transfer model is postulated to explain the relationship between soil–water composition and a_c for the solidified DM. The composition of hydration water, bound water, and pore water is controlled by five parameters: m_{pw0} , m_{bw0} , k_1 , k_2 , and k_3 , where m_{pw0} and m_{bw0} are initial pore water and bound water content, respectively, k_1 and k_2 govern the rate of increment for Δm_{hw} and Δm_{bw} , respectively, which increases with the curing time. k_3 is a fictional bound water content corresponding to a cement content higher than a_{c0} .

The proposed model is used to interpret the mechanical behavior of the solidified DM. Based on the limited experimental data, it is postulated that the brittleness of the solidified DM may be related to the bound water content and the brittle behavior commences when the incremental increase of Δm_{bw} begins decreasing. On the other hand, the unconfined compressive strength of the solidified DM may be related to either Δm_{hw} or Δm_{bw} for $a_c < a_{c0}$ and to Δm_{hw} for $a_c > a_{c0}$.

Acknowledgments

This study is jointly sponsored by the Open Research Fund of State Key Laboratory of Hydrology, Water Resources and Hydraulic Engineering, Hohai University and the National Natural Science Foundation of China through Grant No. 50379011. The diffraction tests were conducted by Professor Li Gang in the Testing and Analysis Center, Nanjing Normal University. Their support is gratefully acknowledged.

Notation

The following symbols are used in this paper:

- a_c = cement content per unit volume (kg/m^3);
- a_{cm} = minimum cement content per unit volume (kg/m^3);
- a_{c0} = threshold cement content per unit volume (kg/m^3);
- c_u = undrained shear strength (kN/m^2);
- h = water head (m);
- k_1 = parameter which controls the rate of hydration water increment (—);
- k_2 = parameter which controls the rate of bound water increment (m^3/kg);
- k_3 = fictional bound water content per unit volume at $a_c > a_{c0}$ (kg/m^3);
- m_{bw} = mass of bound water per unit volume (kg/m^3);
- m_{bw0} = initial mass of bound water per unit volume (kg/m^3);
- m_e = evaporated water content (kg/m^3);
- m_{fw} = mass of free water per unit volume (kg/m^3);
- m_{fw0} = initial mass of free water per unit volume (kg/m^3);
- m_{hw0} = initial mass of hydration water per unit volume (kg/m^3);
- m_{pw} = mass of pore water per unit volume (kg/m^3);
- m_{pw0} = initial mass of pore water per unit volume (kg/m^3);
- q_u = unconfined compressive strength (kN/m^2);

- r_1 = radial distance to the midpoint of the soil specimen in the centrifuge (m);
- r_2 = radial distance to the free water surface in the centrifuge (m);
- Δm_{bw} = increment in mass of bound water per unit volume (kg/m^3);
- Δm_{hw} = increment in mass of hydration water per unit volume (kg/m^3);
- ρ = density of the pore fluid (kg/m^3);
- ψ = soil suction (N/m^2); and
- ω = angular velocity (s^{-1}).

References

- Chew, S. H., Kamruzzaman, A. H. M., and Lee, F. H. (2004). "Physico-chemical and engineering behavior of cement-treated clays." *J. Geotech. Geoenviron. Eng.*, 130(7), 696–706.
- Connor, J. R. (1990). *Chemical fixation and solidification of hazardous wastes*, Van Nostrand Reinhold, New York.
- Dermatas, D., Dadachov, M., Mirabito, M., and Meng, X. (2003a). "Strength development of solidified/stabilized organic waste and optimum treatment design." *J. Air Waste Manage. Assoc.*, 53(11), 1363–1372.
- Dermatas, D., Dutko, P., Balorda-Barone, J., and Moon, D. H. (2003b). "Evaluation of engineering properties of cement treated Hudson River dredged sediments for reuse as fill materials." *J. Marine Environ. Eng.*, 7(2), 101–123.
- Forstner, U., and Calmano, U. (1998). "Characterisation of dredged materials." *Water Sci. Technol.*, 38(11), 149–157.
- Gardner, R. A. (1937). "The method of measuring the capillary tension of soil moisture over a wide moisture range." *Soil Sci.*, 43, 277–283.
- Horpibulsuk, S., Miura, N., and Nagaraj, T. S. (2005). "Clay–water/cement ratio identity for cement admixed soft clays." *J. Geotech. Geoenviron. Eng.*, 131(2), 187–192.
- Joint Committee for Powder Diffraction Standards. (1995). *Index to the powder diffraction file*, International Center for Diffraction Data, Swarthmore, Pa.
- Lea, F. M. (1970). *The chemistry of cement and concrete*, 3rd Ed., Edward Arnold Ltd., London.
- Lee, F. H., Lee, Y., Chew, S. H., and Yong, K. Y. (2005). "Strength and modulus of marine clay–cement mixes." *J. Geotech. Geoenviron. Eng.*, 131(2), 178–186.
- Lebedev, A. F. (1936). *Soil and groundwaters*, The Academy of Sciences of the USSR (in Russian).
- Locat, J., Tremblay, H., and Leroueil, S. (1996). "Mechanical and hydraulic behaviour of a soft inorganic clay treated with lime." *Can. Geotech. J.*, 33, 654–669.
- Meegoda, J. N., et al. (2000). "Re-mediation of chromium contaminated soils—Pilot scale investigation." *Pract. Period. Hazard. Toxic Radioact. Waste Manage.*, 4(1), 7–15.
- Ministry of Construction P. R. China. (1999). "Standard for soil test method." *GB/T 50123-1999*, Beijing (in Chinese).
- Mitchell, J. K. (1981). "Soil improvement state of the art report." *Proc., 10th Int. Conf. on Soil Mechanics and Foundation Engineering*, 4, 509–565.
- Mitchell, J. K., and Soga, K. (2005). *Fundamentals of soil behavior*, 3rd Ed., Wiley, New York.
- Nagaraj, T. S., Miura, N., Yaligar, P. P., and Yamadera, A. (1996). "Predicting strength development by cement admixture based on water content." *Grouting and Deep Mixing: Proc., IS Tokyo '96, 2nd Int. Conf. on Ground Improvement Geosystems*, 431–436.
- Rao, S. N., and Rajasekaran, G. (1996). "Reaction products formed in lime-stabilized marine clays." *J. Geotech. Engrg.*, 122(5), 329–336.
- Tang, Y. X., Miyazaki, Y., and Tsuchida, T. (2001). "Practices of reused dredgings by cement treatment." *Soils Found.*, 41(5), 129–143.

- Tatsuoka, F., Uchida, K., Imai, K., Ouchi, T., and Kohata, Y. (1997). "Properties of cement treated soil in Trans-Tokyo Bay Highway project." *Ground Improvement*, 1(1), 37-57.
- Taylor, H. F. W. (1997). *Cement chemistry*, 2nd Ed., Thomas Telford, London.
- Tremblay, H., Leroueil, S., and Locat, J. (2001). "Mechanical improvement and vertical yield stress prediction of clayey soils from eastern Canada treated with lime or cement." *Can. Geotech. J.*, 38, 567-579.
- Winkels, H. J., and Stein, A. (1997). "Optimal cost-effective sampling for monitoring and dredging of contaminated sediments." *J. Environ. Qual.*, 26(4), 933-946.
- Zhang, H. Q., Xie, J., Zhu, W., Huang, Y. Z., and Shi, P. (2004). "Present situation of dredged materials dumping and the study of transforming dredged mud into regenerative resources—Difficulties of refuses dumping in China seas and countermeasures to deal with these problems." *Bull. Mater. Sci.*, 23(6), 54-60 (in Chinese).